

matic absence of  $h00$  reflections when  $h$  is odd. Therefore, the crystals probably belong to the space group  $P4_232$ .

Although the low resistances of all of these compounds were confirmed by single measurements, only the single crystals of two of them,  $\text{La}(\text{Ni}_{0.5}\text{Ru}_{0.5})\text{O}_3$  and  $\text{La}(\text{Mg}_{0.5}\text{Ru}_{0.5})\text{O}_3$ , were found to be sufficiently large and well-shaped so that platinum paste electrodes could be applied to the faces and extensive electrical resistivity measurements made. The former cubic crystals were 2 mm. on an edge while the latter were 1 mm. on an edge. A constant current was applied and the voltage drop was measured across a standard resistor in series with the crystal. The plots of log resistivity vs.  $1000/T$  for  $\text{La}(\text{Ni}_{0.5}\text{Ru}_{0.5})\text{O}_3$  and  $\text{La}(\text{Mg}_{0.5}\text{Ru}_{0.5})\text{O}_3$  shown in Figure 1 are typical of semiconductors. Calculations from these plots show that the conduction activation energies for these compounds are 0.120 and 0.046 e.v., respectively.

### Conclusions

The growth of single crystals of several complex

perovskite-type compounds, although the crystals are not large, is a step toward obtaining many of these materials in a suitable form for good electrical measurements. Crystals of  $\text{La}(\text{Ni}_{0.5}\text{Ru}_{0.5})\text{O}_3$  and  $\text{La}(\text{Mg}_{0.5}\text{Ru}_{0.5})\text{O}_3$ , for instance, were large enough to make meaningful resistivity measurements. It is realized that other techniques of crystal growing besides the flux technique may produce larger crystals of complex perovskite-type compounds. In this connection, investigations of growing these crystals by the Czochralski and Verneuil techniques are presently being conducted at the Research Laboratories.

**Acknowledgment.**—The authors wish to thank Bernarr Jacob and Valentine Patarini for their assistance in crystal growing and making electrical measurements.

CONTRIBUTION FROM THE BAKER LABORATORY OF CHEMISTRY,  
CORNELL UNIVERSITY, ITHACA, NEW YORK

## Solid State Studies of Tungsten Trioxide Single Crystals below Room Temperature<sup>1</sup>

BY BILLY LEE CROWDER AND M. J. SIENKO

Received August 7, 1964

The Hall voltage, electrical resistivity, and thermoelectric power have been measured as a function of temperature on single crystals of  $\text{WO}_3$  in the range 140–300°K. Discontinuities appear on cooling at approximately +10 and –40°, corresponding, respectively, to a monoclinic-to-triclinic ( $\gamma$ -to- $\beta$ ) and a piezoelectric-to-ferroelectric ( $\beta$ -to- $\alpha$ ) transition. The  $\gamma$ -to- $\beta$  transition is strongly dependent on the domain characteristics and the impurity concentrations of the individual crystals. Introduction of oxygen vacancies leads to disappearance of the discontinuities at +10 and –40°.

### Introduction

Tungstic oxide is the host structure for the "tungsten bronzes,"  $\text{M}_x\text{WO}_3$  ( $0 < x < 1$ ). The solid state properties of  $\text{WO}_3$  are of interest, since the metallic properties of the tungsten bronzes can be interpreted in terms of a quasi-free-electron model in which a d-orbital conduction band of the host  $\text{WO}_3$  is populated by electrons from donor atoms M.<sup>2</sup> In the case of the alkali tungsten bronzes with  $x > 0.25$ , the donor ionization energy is apparently very small and may even be zero,<sup>3</sup> but in the copper tungsten bronzes<sup>4</sup> the donor ionization energy seems to be large enough compared to the thermal energy to produce semiconducting behavior below about 220°K. Single crystal studies of  $\text{Cu}_x\text{WO}_3$  by electrical conductivity, Hall voltage, and thermoelectric power measurements disclose, however, anomalously low carrier densities. Also, there are marked changes in specific resistivity which have been assigned to major changes in carrier mobility brought about by phase changes in the host structure. Similar resistivity

behavior has been observed in single crystals of  $\text{Ag}_x\text{WO}_3$ .<sup>5</sup> The present investigation was undertaken to elucidate the carrier characteristics in the conduction band of the  $\text{WO}_3$  host structure. This paper reports the results obtained below room temperature. Results obtained above room temperature have been reported previously.<sup>6</sup>

$\text{WO}_3$  can exist in antiferroelectric<sup>7</sup> as well as ferroelectric modifications<sup>8</sup> and shows several other transitions at which changes occur in domain structure,<sup>9–11</sup> optical indices of refraction,<sup>12</sup> dielectric constant,<sup>8,9</sup> "thermal transition of transparency,"<sup>13</sup> optical absorption edge,<sup>14</sup> specific heat,<sup>10</sup> coefficient of expansion,<sup>15</sup> and electrical conductivity.<sup>9,16</sup> Figure 1 summarizes the relations of the four phases that have been defined, including the hysteresis effects noted.

(5) M. J. Sienko and B. R. Mazumder, *J. Am. Chem. Soc.*, **82**, 3508 (1960).

(6) B. L. Crowder and M. J. Sienko, *J. Chem. Phys.*, **38**, 1576 (1963).

(7) W. L. Kehl, R. G. Hay, and D. Wahl, *J. Appl. Phys.*, **23**, 212 (1952).

(8) B. T. Matthias, *Phys. Rev.*, **76**, 430 (1949).

(9) S. Sawada, *J. Phys. Soc. Japan*, **11**, 1237 (1956).

(10) S. Sawada and G. C. Danielson, *Phys. Rev.*, **113**, 1005 (1959).

(11) S. Tanisaki, *J. Phys. Soc. Japan*, **15**, 566 (1960).

(12) S. Sawada and G. C. Danielson, *Phys. Rev.*, **113**, 1008 (1959).

(13) T. Horie, K. Kawabe, and T. Iwai, *Ann. Rept. Sci. Works, Fac. Sci., Osaka Univ.*, **4**, 45 (1958).

(14) T. Iwai, *J. Phys. Soc. Japan*, **15**, 1596 (1960).

(15) M. Foëx, *Compt. rend.*, **220**, 917 (1945); **228**, 1335 (1949).

(16) S. Sawada and G. C. Danielson, *Phys. Rev.*, **113**, 803 (1959).

(1) This research was sponsored by the Air Force Office of Scientific Research under grant AF-AFOSR-62-218 and was supported in part by the Advanced Research Projects Agency. This report is based on the Ph.D. thesis of B. L. Crowder.

(2) M. J. Sienko, *Advances in Chemistry Series*, No. 30, American Chemical Society, Washington, D. C., 1963, p. 224.

(3) M. J. Sienko and T. B. N. Truong, *J. Am. Chem. Soc.*, **83**, 3930 (1961).

(4) M. J. Sienko and P. F. Weller, *Inorg. Chem.*, **1**, 324 (1962).

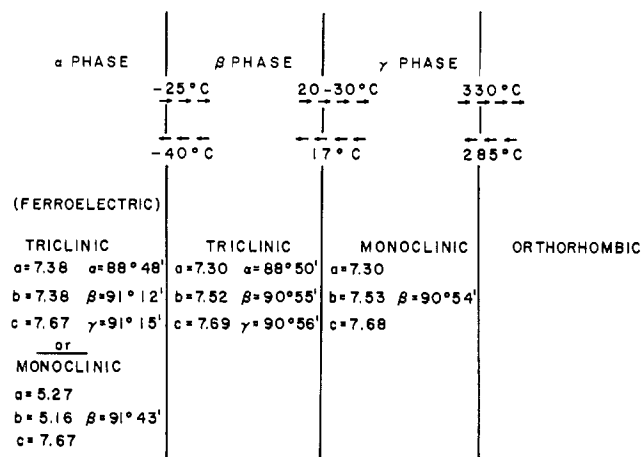


Figure 1.—Phase relations for tungstic oxide.

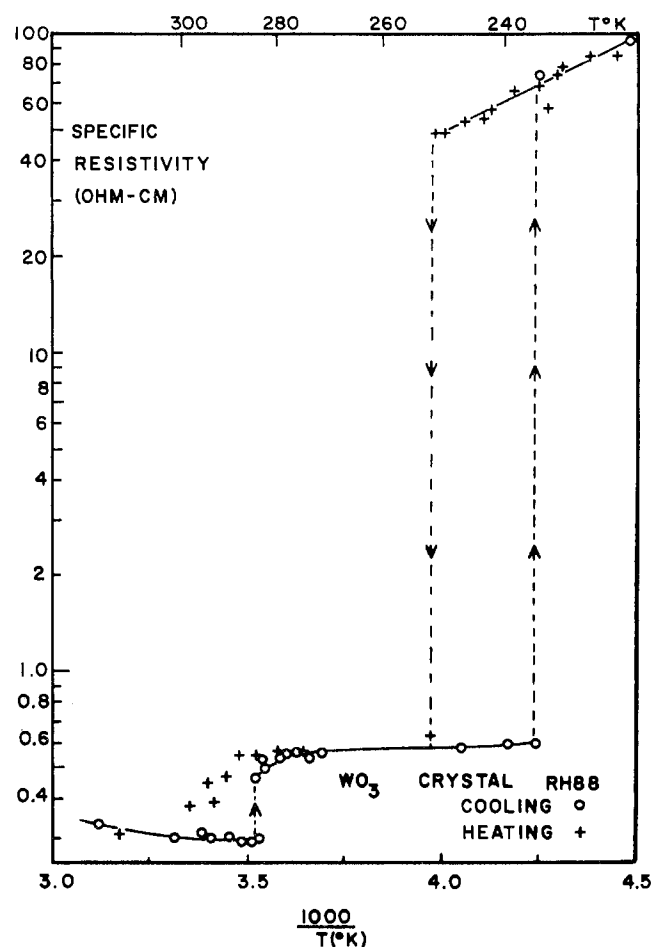
### Experimental

**Preparation.**—Single crystals of  $WO_3$  were prepared by heating Fisher "purified" tungstic anhydride for 4–7 days at about 1350° in platinum. The crystals grew on the inside surface of the platinum and, occasionally, in the bulk powder. Spectroscopic analysis indicated 0.0001% Cu, 0.1% U, and (in the more highly conducting crystals) 0.001% In. Many of the crystals from the vapor phase growth were directly suitable for measurement; others, including those grown in the bulk powder, had to be cleaved. Specimens varied from  $1 \times 0.5 \times 0.3$  mm.<sup>3</sup> to  $3 \times 1 \times 0.5$  mm.<sup>3</sup>. All of the crystals showed, on petrographic examination, the domain characteristics previously reported.<sup>9–11</sup> A few of the crystals were subjected to slight pressure to convert them to single-domain crystals at room temperature. No observable changes in domain structure or in electrical properties were noted on annealing the crystals in air in platinum at 500° for a few days.

Oxygen-deficient  $WO_3$  was prepared by heating single crystals of  $WO_3$  under vacuum at various temperatures. Electrical measurements before and after such treatment and after subsequent heating in air indicated that the oxygen loss is a reversible process. To verify that the oxygen loss is a bulk effect, the faces of one treated crystal were cleaved off and the crystal remeasured; no marked changes were observed in either the magnitude of the specific resistivity or its temperature dependence.

**Hall Voltage Measurements.**—Current was passed through the crystal *via* indium-faced brass contact screws. Two 7-mil tungsten wires, sharpened in molten sodium nitrite, pressed against one side of the crystal to furnish a pair of potential probes (for resistivity measurements) and also a virtual Hall probe. A knife edge of chromel A against the opposite face of the crystal furnished the other Hall probe. Because the domain structure of  $WO_3$  is sensitive to pressure, the pressure contacts were on occasion replaced by tiny globs of gallium on fine silver wire, giving pressureless contacts of less precisely defined probe separation. Temperature variation was produced by immersion in a cryogenic bath or by varying the inlet flow of nitrogen gas from a copper coil immersed in liquid nitrogen or acetone–Dry Ice. Most of the measurements were done with the chopper technique of Dauphinee and Mooser.<sup>17</sup> To eliminate d.c. effects, the circuit was used with a square wave of 38 c.p.s. The magnetic field was produced by a 4-in. electromagnet powered by a Varian 2100A supply. A field of 6700 gauss, homogeneous to within 1 gauss over the sample volume and calibrated with proton resonance, was employed in most of the measurements. In each case, Hall voltage was determined for both field directions. Sample dimensions, measured microscopically through a graduated ocular that had been calibrated with a stage micrometer, were fixed to at least 1%.

**Thermoelectric Power.**—The thermal gradient (generally about 2°) was supplied by a wire-wound resistance heater at one

Figure 2.—Log of specific resistivity vs. reciprocal temperature as observed by dynamic measurements on a single crystal of  $WO_3$ .

end of the crystal and a brass-block heat sink at the other. Thermal contact between the crystal and the heat source-and-sink was provided by indium–mercury amalgam or by gallium. The thermal gradient was determined by measuring the temperature at two points on the crystal with copper–constantan thermocouples attached to the crystal; the thermal e.m.f., by measuring the voltage drop across the two copper leads of the thermocouples. For measurements, the crystal holder was surrounded by a radiation shield and placed in a Pyrex tube which was evacuated to about  $10^{-3}$  torr. Temperature control was obtained by immersing the Pyrex tube in various baths and by varying the input voltage to the radiation shield heater.

**Resistivity.**—In addition to static resistivity measurements in the holders above, using either the tungsten probes of the Hall effect holder or the copper legs of the thermocouples in the thermoelectric power holder as potential probes, dynamic measurements were made to monitor the resistance continuously as the temperature varied through the phase transitions. For this purpose, a crystal was pressed by a weak phosphor bronze spring against parallel silver wires lying on a mica sheet (placed over a mass of copper). Gallium on the ends of the crystal furnished current contacts; condenser discharge between the silver wires and the crystal "formed" potential probe contacts. Constant current was maintained through the crystal while the potential drop between the silver probes was continuously recorded with a potentiometric recorder. A copper–constantan thermocouple immediately adjacent to the crystal was monitored simultaneously on a potentiometric recorder. For the cooling cycles, the holder was placed in an evacuated Pyrex tube which was immersed in a Dry Ice–acetone bath while power input to a radiation shield around the crystal holder was slowly reduced through a

(17) T. M. Dauphinee and E. Mooser, *Rev. Sci. Instr.*, **26**, 660 (1955).

motor-driven rheostat. About 4 hr. was taken to go from room temperature to  $-60^\circ$ .

**Results**

Figure 2 represents the recorder course of a typical crystal of  $WO_3$  in its resistivity behavior on successive cooling and warming cycles. On cooling, there is first a slight decrease in resistivity followed by a discontinuous increase (in one step at  $+10^\circ$  for single-domain crystals or in several steps in the range  $+10$  to  $-10^\circ$  for poly-domain specimens) to a value some two or three times as large as the room temperature value. This change is ascribable to the  $\gamma$ -to- $\beta$  phase transition. A second, more marked discontinuous rise, by a factor of about  $10^2$ , occurs in the neighborhood of  $-36$  to  $-40^\circ$  and is ascribed to the  $\beta$ -to- $\alpha$  transition. On warming, there is a linear decrease in the logarithm of the specific resistivity *vs.* reciprocal temperature with an abrupt decrease by about two orders of magnitude in specific resistivity at  $-22^\circ$ . On further warming, the resistance decreases slowly until the region for the  $\beta$ -to- $\gamma$  transition is reached. This transition always occurred over a wide temperature range, starting at about  $17^\circ$  and extending to  $20$  or  $30^\circ$ . On repeated cooling and heating cycles, the above hysteresis effects reproduced themselves. Figures 3 and 4 represent static measurements of resistivity on two other crystals of  $WO_3$ , the crystal in Figure 3 starting as a single domain at room

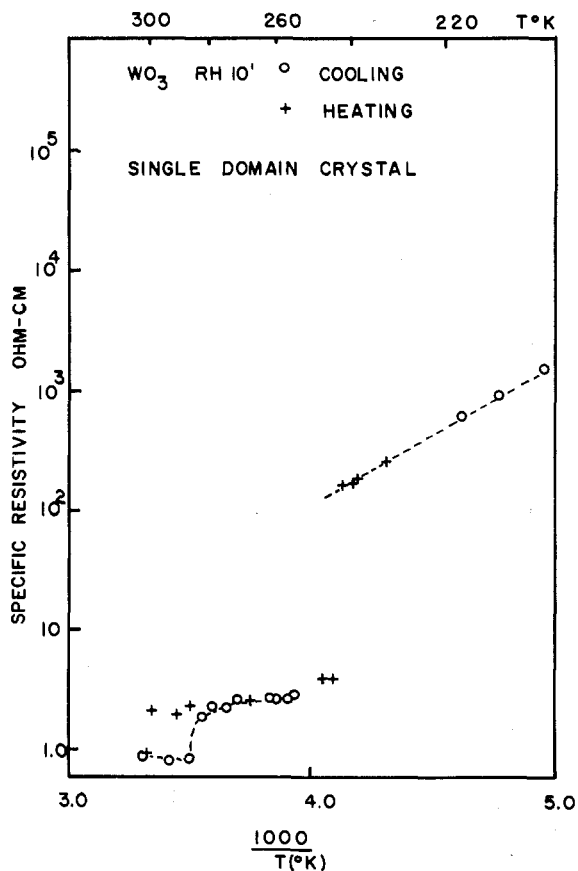


Figure 3.—Log of specific resistivity *vs.* reciprocal temperature as observed by static measurements on a single-domain crystal of  $WO_3$ .

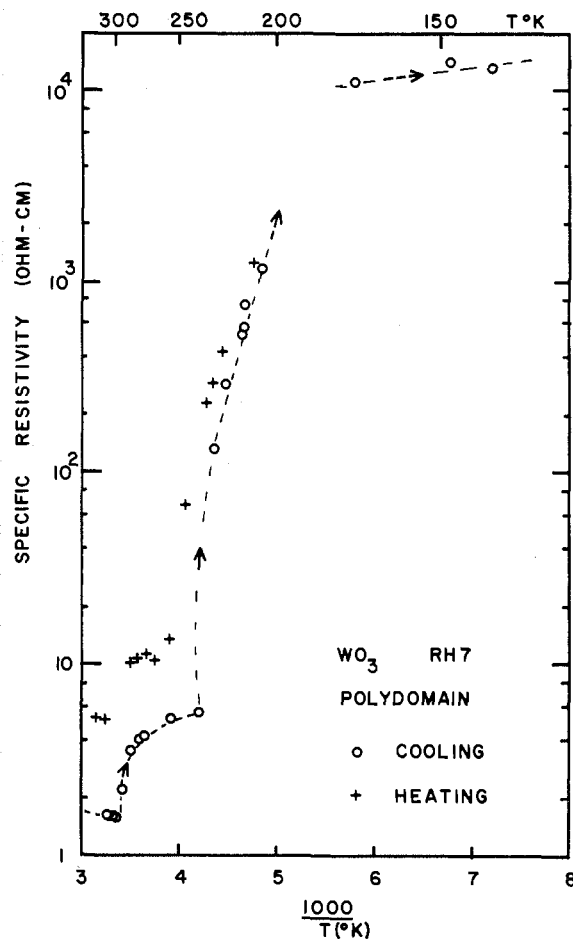


Figure 4.—Log of specific resistivity *vs.* reciprocal temperature as observed by static measurements on a poly-domain crystal of  $WO_3$ .

temperature and the one in Figure 4 as a poly-domain crystal.

Typical thermoelectric power results are presented as a function of temperature in Figure 5. This typifies the single-domain case, referring in fact to the same crystal as represented in Figure 3. As with the resistivity, discontinuities appear in the thermoelectric power at temperatures corresponding to the  $\gamma$ - $\beta$  and  $\beta$ - $\alpha$  phase changes. Hysteresis between cooling and heating cycles is again evident.

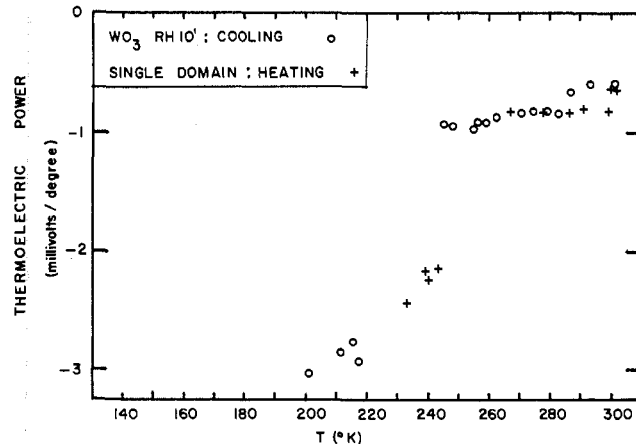


Figure 5.—Thermoelectric power *vs.* temperature for a single-domain crystal of  $WO_3$ .

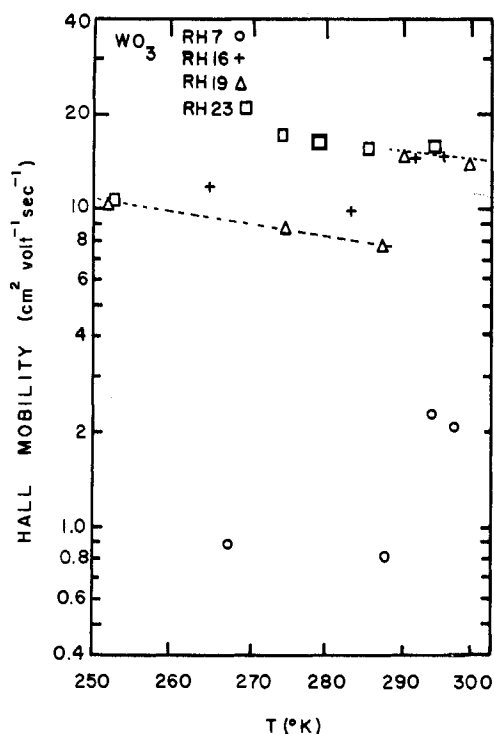


Figure 6.—Hall mobility vs. temperature for several crystals of  $\text{WO}_3$  in the vicinity of the  $\beta$ -to- $\gamma$  transition. (The dotted curve is calculated assuming the mobility discontinuity is due entirely to change in effective mass.)

The Hall voltage could not be measured at temperatures below that corresponding to the  $\beta$ - $\alpha$  transition. (It may be that the carrier mobility in the  $\alpha$  phase is too low to produce a favorable signal-to-noise ratio.) In the region of the  $\gamma$ -to- $\beta$  transition, there is typically a twofold drop in the Hall mobility (defined as the product of the Hall coefficient  $R_H$  and the specific conductivity  $\sigma$ ). Results for four crystals are shown in Figure 6. Crystal RH 23 exhibited unusual behavior in that the break in specific resistivity, normally occurring at about  $+10^\circ$ , did not occur until the temperature was about  $-10^\circ$ . This unusual behavior was reproducible.

Oxygen-deficient crystals exhibit behavior which is quite different from that of as-grown  $\text{WO}_3$  crystals, in that both the discontinuity at the  $\gamma$ -to- $\beta$  transition temperature and that at the  $\beta$ -to- $\alpha$  transition temperature disappear. For example, a reduced crystal (prepared by heating under vacuum at  $350^\circ$  for 220 hr.) showed a linear decrease in thermoelectric power from  $-650 \mu\text{volts}$  at  $300^\circ\text{K}$ . to  $-900 \mu\text{volts}$  at  $140^\circ\text{K}$ . The specific resistivity of this particular specimen was 0.14 ohm cm. at room temperature. The Hall coefficient increased monotonically in absolute value as the temperature decreased, changing from  $-0.7 \text{ cc./coulomb}$  at  $300^\circ\text{K}$ . to  $-1.7 \text{ cc./coulomb}$  at  $200^\circ\text{K}$ . The  $\text{WO}_3$  single crystal from which this reduced specimen was obtained had a room temperature specific resistivity of 0.69 ohm cm. and a Hall coefficient of  $-2.8 \text{ cc./coulomb}$ . Thus, the vacuum treatment reduced the resistivity and the Hall voltage by a factor of approximately five but left the mobility essentially unchanged.

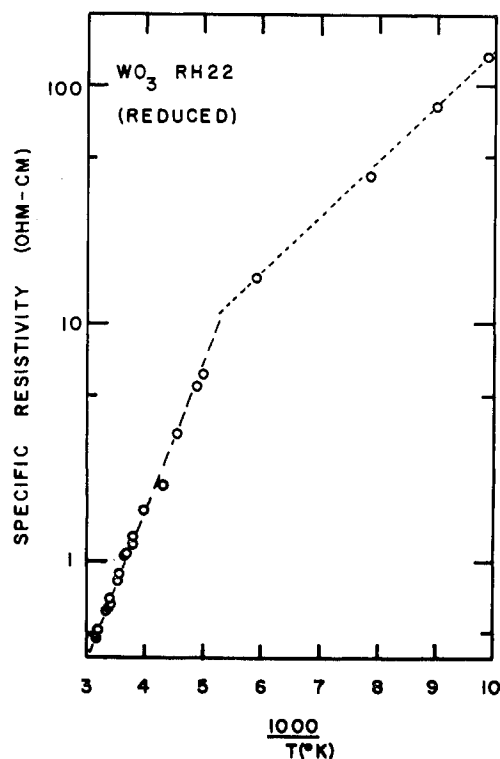


Figure 7.—Log of specific resistivity vs. reciprocal temperature for an oxygen-deficient crystal of  $\text{WO}_3$ .

Figure 7 shows the temperature variation of the resistivity of an oxygen-deficient crystal, prepared by heating a crystal under vacuum at  $800^\circ$  for 72 hr. The thermoelectric power (*vs.* copper) of this reduced specimen was  $-190 \mu\text{volts/deg.}$  at  $290^\circ\text{K}$ .

#### Discussion

A quantitative explanation of the electrical properties in the  $\beta$  and  $\alpha$  phases of  $\text{WO}_3$  is complicated by lack of information on the parameters used so successfully in analyzing the behavior in the  $\gamma$  phase.<sup>6</sup> The change in specific resistivity that occurs at the  $\gamma$ -to- $\beta$  phase transition is primarily due to a decrease in carrier mobility. There is a slight change in the Hall coefficient and a slight increase in its temperature dependence. These small changes suggest there is also a slight increase in the donor ionization energy, probably caused by the slight structure rearrangement (leading to a change in the Madelung potential at an interstitial site). The most significant change, however, is in the mobility.

A decrease in carrier mobility can arise from (1) a change in the scattering mechanisms, (2) an increase in the carrier effective mass, or a combination of both. The dotted curves drawn in Figure 6 have been calculated on the assumption that the decrease in mobility is due entirely to a change in effective mass. The analysis, along the lines of ref. 6, assumes that the mobility in the  $\gamma$  phase is due primarily to polar scattering by optical mode lattice vibrations with a small contribution from neutral impurity scattering. The polaron mass is about  $1.2 m$  for  $\gamma\text{-WO}_3$ ; the observed discontinuity requires the polaron mass to be about  $2.1 m$  in the  $\beta$  phase.

The observed increase in the absolute magnitude of the thermoelectric power at the  $\gamma$ -to- $\beta$  transition is a little too large to be accounted for by the above increase in effective mass and by the slight increase in carrier concentration. In addition, the magnitude of the thermoelectric power increases at a rate faster than that predicted. These observations imply that an additional scattering mechanism is also required to explain the thermoelectric power results.

$\gamma$ - $\text{WO}_3$  is centrosymmetric<sup>18</sup>; the  $\beta$  phase is not.<sup>11</sup> The phase transition, which corresponds to very small distortions of the pseudocubic  $\gamma$ - $\text{WO}_3$ , can therefore provide the necessary additional scattering mechanism; *i.e.*, polar scattering by acoustical mode piezoelectric phonons.<sup>19</sup> This mechanism alone can provide both an explanation of the break in the specific resistivity, which is then due to the increased electron scattering, and the discontinuity in thermoelectric power, which is attributable to a phonon-drag contribution caused by the piezoelectric scattering mechanism (as in ZnO and CdS<sup>19</sup>). In addition, the increase in thermoelectric power with decreasing temperature (over and above the increase due to decreasing carrier concentration) is explained. A difficulty with this explanation, however, is that it requires the piezoelectric effect to be very large for  $\beta$ - $\text{WO}_3$ .

The marked discontinuity in the specific resistivity which occurs in the  $\beta$ -to- $\alpha$  transition may be indicative of a marked decrease in carrier concentration or of a marked decrease in carrier mobility. Without a measurement of the Hall coefficient in the  $\alpha$  phase, it is difficult to separate the two possibilities. Assuming that the donor level concentration is not markedly affected by the phase transition, it is still possible that there might be a marked change in the density of free carriers if the donor ionization energy were drastically changed (as by a marked change in the Madelung potential at an inter-

stitial site). It would seem that the thermoelectric power in the  $\alpha$  phase is much too large to be accounted for by the electron concentration change without resorting to an enormous effective mass which is a strong function of temperature. Therefore, it is extremely probable that a large phonon-drag contribution occurs in the  $\alpha$  phase. In view of the fact that  $\alpha$ - $\text{WO}_3$  is ferroelectric, the presence of a large phonon-drag effect would not be at all surprising.

The above analysis does not take into account that the domain structure changes at each phase transition, the number of domains increasing on going from the  $\gamma$  phase to the  $\beta$  phase to the  $\alpha$  phase.<sup>11</sup> Scattering at domain boundaries could be another significant factor in reducing carrier mobility.

Removal of oxygen to produce oxygen-deficient  $\text{WO}_3$  leads to results qualitatively different from those characteristic of as-grown  $\text{WO}_3$ . Therefore, we conclude that the donor centers responsible for the behavior of as-grown  $\text{WO}_3$  are not primarily oxygen deficiencies. If enough oxygen is removed from the  $\text{WO}_3$  structure, the discontinuities in electrical properties corresponding to the phase transitions do not occur. Since  $\alpha$ - $\text{WO}_3$  is ferroelectric, this observation might be of interest in the theory of ferroelectricity, where the transition to the ferroelectric state (in the perovskite ferroelectrics) is believed to be a cooperative phenomenon.

From the observed thermoelectric power for the oxygen-deficient crystal described in the Results section we estimate the electron concentration (assuming the effective mass equals the electron rest mass) to be about  $10^{19}$  cm.<sup>-3</sup>. This implies that the number of oxygen vacancies is about  $10^{21}$  cm.<sup>-3</sup>—that is, about one oxygen atom in fifty has been removed. In this particular specimen, the number of donor states before reduction was about  $10^{18}$  cm.<sup>-3</sup>. The presence of these shallow centers is believed to account for the change in slope in Figure 7 at lower temperatures.

(18) S. Tanisaki, *J. Phys. Soc. Japan*, **15**, 573 (1960).

(19) A. R. Hutson, *J. Appl. Phys.*, **32**, 2287 (1961).